Probing photonic content of the proton using photon-induced dilepton production in $p + \mathrm{Pb}$ collisions at the LHC

M. Dyndal and A. Glazov

DESY

M. Luszczak and R. Sadykov

.

Abstract

We propose a new experimental method to validate photon parton distribution function (PDF) inside the proton at LHC energies. It is based on the measurement of dilepton production from the $\gamma p \to \ell^+\ell^- + X$ reaction in proton–lead collisions. These experimental conditions guarantee relatively clean environment, both in terms of reconstruction of the final state and in terms of possible background. We firstly calculate the cross sections for this process with collinear photon PDFs, where we identify correct choice of the scale, in analogy to deep inelastic scattering kinematics. We then include the virtuality of probed photon in the calculations, based on modern parameterizations of deep inelastic structure functions. Finally, we find that significant rates of this process are accessible by LHC experiments with existing datasets.

I. INTRODUCTION

Precise calculations of various electroweak reactions in pp collisions at the LHC need to account for, on top of the higher-order corrections, the effects of photon-induced subprocesses. The relevant examples are the production of lepton pairs [1–5] or pairs of electroweak bosons [6–13].

Recently, a precise photon distribution inside the proton has been evaluated in Ref. [14]. This approach provides a model-independent determination of the photon PDF (embedded in so-called LUXqed distribution) and it is based on proton structure function and elastic form factor fits in electron–proton scattering.

Up to date, there are no experimentally clean processes identified that would allow to either strongly constrain or verify the calculations. For example, the extraction of photon PDF from isolated photon production in deep inelastic scattering (DIS) [15] or from inclusive $pp \to \ell^+\ell^- + X$ reaction [2, 16, 17] is limited due to large QCD background. On contrary, the elastic part of the photon PDF is verified via exclusive $\gamma\gamma \to \ell^+\ell^-$ process, measured in pp collisions by ATLAS [18, 19], CMS [20, 21] and recently by CMS+TOTEM [22] collaborations.

We therefore propose a new experimental method to constrain photonic content of the proton. Thanks to the large fluxes of quasi-real photons from the Pb ion at the LHC, the photon-induced dilepton production in $p + \mathrm{Pb}$ collision configuration is a very clean way to probe photon PDF. This process is shown schematically in Fig. 1, where by analogy to DIS, two leading-order diagrams can be identified. Since the photon flux from the ion scales with Z^2 and QCD-induced cross-sections scale approximately with A, the amount of QCD background is greatly reduced comparing to pp case.

Moreover, as this process does not involve the exchange of color with the photon-emitting nucleus, no significant particle production is expected in the rapidity region between the dilepton system and the nucleus. The photon-emitting nucleus is also expected to produce no neutrons because the photons couple to the entire nucleus. Thus, a combination of a rapidity gap and zero neutrons in the same direction provide straightforward criteria to identify these events experimentally.

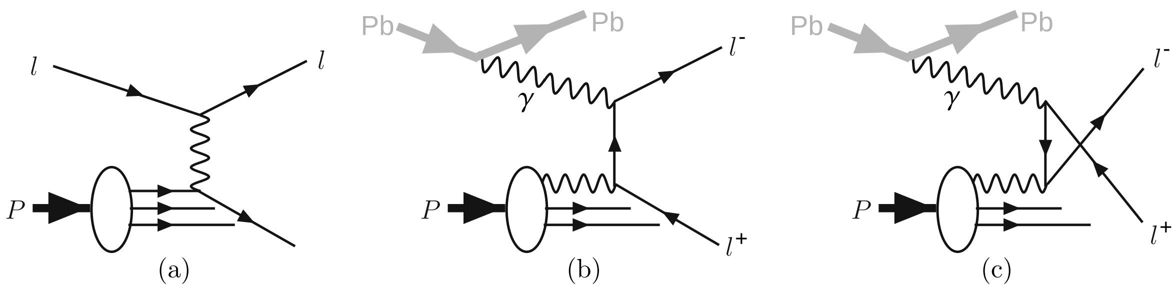

FIG. 1: Schematic graphs for deep inelastic scattering, $\ell^{\pm}p \to \ell^{\pm} + X$ (a) and photon-induced dilepton prodcution, $\gamma p \to \ell^{+}\ell^{-} + X$, in $p+$Pb collisions for t-channel (b) and u-channel (c) lepton exchange.

II. FORMALISM

A. Elastic photon fluxes

To get the distribution of the elastic photons from the proton, one can express the equivalent photon flux through the electric and magnetic form factors $G_E(Q^2)$ and $G_M(Q^2)$ of the proton. This contribution is obtained as

$$\gamma^{p}_{el}(x,Q^2) = \frac{\alpha_{\rm em}}{\pi}\left[\left(1-\frac{x}{2}\right)^2 \frac{4m_p^2 G_E^2(Q^2) + Q^2 G_M^2(Q^2)}{4m_p^2 + Q^2} + \frac{x^2}{4} G_M^2(Q^2)\right] , \tag{1}$$

where x is the momentum fraction of the proton taken by the photon, Q^2 is the photon virtuality, $\alpha_{\rm em}$ is the electromagnetic structure constant and m_p is the proton mass.

To express the elastic photon flux for the nucleus ($\gamma^{\rm Pb}_{el}$), we follow Ref. [23] and replace

$$\frac{4m_p^2 G_E^2(Q^2) + Q^2 G_M^2(Q^2)}{4m_p^2 + Q^2} \longrightarrow Z^2 F^2_{\rm em}(Q^2) , \tag{2}$$

where $F_{\rm em}(Q^2)$ is the electromagnetic formfactor of the nucleus and Z is its charge. We also neglect the magnetic formfactor of the ion in the following (it even rigorously vanishes for spinless nuclei).

For the Pb nucleus, we use the formfactor parameterization from the STARlight MC generator [24]:

$$F_{\rm em}(Q^2) = \frac{3}{(QR_A)^3}\Big[\sin(QR_A) - QR_A\cos(QR_A)\Big]\frac{1}{1+a^2Q^2} , \tag{3}$$

where $R_A = 1.1A^{1/3}$ fm, $a = 0.7$ fm and $Q = \sqrt{Q^2}$.

B. Collinear-factorization approach and choice of the scale

The inelastic processes, with breakup of a proton, can be also considered. At LO and at a given scale μ^2, the photon parton distribution $\gamma^p_{inel}(x,\mu^2)$ of photons carrying a fraction z of the proton's momentum, obeys the DGLAP equation:

$$\frac{d\gamma^p_{inel}(x,\mu^2)}{d\log\mu^2} = \frac{\alpha_{\rm em}}{2\pi}\int_x^1 \frac{dy}{y}\Big[\sum_q e_q^2 P_{\gamma\leftarrow q}(y) q(\frac{x}{y},\mu^2) + P_{\gamma\leftarrow\gamma}(y)\gamma^p_{inel}(\frac{x}{y},\mu^2)\Big] \,, \tag{4}$$

where $q(x,\mu^2)$ is the quark PDF, e_q is the quark charge, $P_{\gamma\leftarrow q}$ is the $q\to\gamma$ splitting function, and $P_{\gamma\leftarrow\gamma}$ corresponds to the virtual self-energy correction to the photon propagator. This is the basis for collinear photon-PDF determination in all initial [25, 26] and more recent [14, 16, 17, 27–30] considerations.

However, none of these studies identify the prescription for the choice of the scale μ^2, which is needed to calculate the cross section for the process of interest. The usual choice for μ is the mass of the system from hard interaction, or the transverse momentum of the leading object. By analogy to DIS (Fig. 1), where the scale is associated with the virtuality of the exchanged photon, it is possible to define the scale in case of the $\gamma\gamma\to\ell^+\ell^-$ process. This is achieved by taking the virtuality of massive t- or u-channel propagator (Fig. 1b or c). Hence, $\mu = p_T^{\ell^-}$ for t-channel diagram and $\mu = p_T^{\ell^+}$ for t-channel exchange. One should note, however, that t/u channel diagrams cannot be separated experimentally. In this case, on can use the average p_T of the leptons with appropriate uncertainty.

In the collinear approach, the $p+\mathrm{Pb}\to\mathrm{Pb}+\ell^+\ell^-+X$ production cross section can be written as

$$\sigma = S^2\int dx_p dx_{\rm Pb}\Big[\left(\gamma^p_{el}(x_p)+\gamma^p_{inel}(x_p,\mu^2)\right)\gamma^{\rm Pb}_{el}(x_{\rm Pb})\sigma_{\gamma\gamma\to\ell^+\ell^-}(x_p,x_{\rm Pb})\Big] \,, \tag{5}$$

where $\sigma_{\gamma\gamma\to\ell^+\ell^-}$ is the elementary cross section for the $\gamma\gamma\to\ell^+\ell^-$ subprocess and S^2 is the so-called survival factor which takes into account the requirement that there be no hadronic interactions between the proton and the ion.

C. k_T-factorization approach

At lowest order, the calculations with collinear photons produce leptons that are back-to-back in transverse kinematics. Therefore, to take the effect of transverse momentum smearing into account, a dedicated parton shower algorithms are usually used.

In the k_T factorization approach, one can parametrize the $\gamma^* p \to X$ vertices in terms of the proton structure functions. The photons from inelastic production have transverse momenta and non-zero virtualities Q^2 and the unintegrated photon distributions are used, in contrast to collinear distributions. In the DIS limit, the unintegrated inelastic photon flux can be obtained using the following equation [4, 31]:

$$\frac{d\gamma^p_{inel}(x,Q^2)}{d\log Q^2} = \frac{\alpha_{\rm em}}{2\pi}\int_x^1 \frac{dy}{y} P_{\gamma\leftarrow q}(\frac{x}{y})\frac{F_2(y,Q^2)}{y}\left(1-\frac{x}{y}\right) , \tag{6}$$

where $F_2(x,Q^2)$ is the standard proton structure function, and the splitting function $P_{\gamma\leftarrow q}(x)$ is given as

$$P_{\gamma\leftarrow q}(x) = \frac{1+(1-x)^2}{x} \tag{7}$$

These unintegrated fluxes enter the $p+\mathrm{Pb}\to\mathrm{Pb}+\ell^+\ell^-+X$ production cross section as

$$\sigma = S^2\int dx_p dx_{\rm Pb} d\vec{q_T}\Big[\left(\gamma^p_{el}(x_p,Q^2)+\gamma^p_{inel}(x_p,Q^2)\right)\gamma^{\rm Pb}_{el}(x_{\rm Pb})\sigma_{\gamma^*\gamma\to\ell^+\ell^-}(x_p,x_{\rm Pb},\vec{q_T})\Big] , \tag{8}$$

where $\sigma_{\gamma^*\gamma\to\ell^+\ell^-}$ is the off-shell elementary cross-section [31] and $\vec{q_T}^2 = Q^2$.

III. EXAMPLE EXPERIMENTAL CONFIGURATION AND POSSIBLE BACKGROUND SOURCES

We assume collision setup from recent $p+\mathrm{Pb}$ run at the LHC, carried out at the centre-of-mass energy per nucleon pair $\sqrt{s_{NN}}$ = 8.16 TeV. Since the energy per nucleon in the proton beam is larger than in the lead beam, the nucleon–nucleon centre-of-mass system has a rapidity in the laboratory frame of +0.465.

As an example of method's applicability, we will use the geometry of ATLAS [32] and CMS [33] detectors in the following. We also consider dimuon-channel only, however the integrated results for ee and $\mu\mu$ channels can be obtained by simply multiplying all cross-sections by a factor of two.

We start with applying minimum transverse momentum requirement of 4 GeV to both muons. This requirement is imposed to ensure high lepton reconstruction and triggering efficiency. Moreover, due to limited acceptance of the detectors, each muon is required to

Variable	Requirement
lepton transverse momentum, p_{T}^{ℓ}	> 4 GeV
lepton pseudorapidity, $\lvert\eta^{\ell}\rvert$	< 2.4
dilepton invariant mass, $m_{\ell^+\ell^-}$	> 10 GeV

TABLE I: Definition of the fiducial region used in the studies.

have a pseudorapidity (η^{ℓ}) that satisfies $|\eta^{\ell}| < 2.4$ condition. Our calculations are carried out for a minimum dilepton invariant mass of $m_{\ell^+\ell^-} = 10$ GeV. Such a choice is due to removal of possible contamination from $\Upsilon(\to \ell^+\ell^-)$ photoproduction process. Summary of all selection requirements is presented in Table I

Possible background for this process can arise from inclusive lepton-pair production, e.g. from Drell–Yan process [34–37]. This processes would lead to disintegration of the incoming ion, and zero-degree calorimeters (ZDC) [38, 39] can be used to veto very-forward-going neutral fragments which would allow to fully reduce this background. Another background can arise from diffractive interactions, hence possibly mimicking signal topology. However, since the nucleus is a fragile object (with the nucleon binding energy of just 8 MeV) even the softest diffractive interaction will likely result in the emission of a few nucleons from the ion, detectable in the ZDC.

Another background category is the photon-induced process with resolved photon, i.e. $\gamma p \to Z/\gamma^* + X$ reaction. Here, the rapidity gap is expected to be smaller than in the signal process due to the additional particle production associated with the "photon remnant". Any other residual contamination of this process can be controlled using dedicated region, with a dilepton invariant mass around the Z-boson mass.

IV. RESULTS WITH COLLINEAR PHOTON-PDFS

We start with the calculation of the elastic contribution, $p + \mathrm{Pb} \to p + \mathrm{Pb} + \ell^+\ell^-$. In this case the photon flux becomes:

$$\gamma_{el}^{p}(x, Q^2) = \gamma_{el}^{p}(x) \tag{9}$$

and the following parameterization is used [23]:

$$\gamma^p_{el}(x) = \frac{\alpha_{\rm em}}{\pi}\left(\frac{1-x+0.5x^2}{x}\right)\left(\frac{A+3}{A-1}\log A - \frac{17}{6} - \frac{4}{3A} + \frac{1}{6A^2}\right) , \qquad (10)$$

where $A = 1 + \frac{Q_0^2(1-x)}{xm_p^2}$ and $Q_0^2 = 0.71$ GeV^2. This parameterization is a good analytical approximation of Eq. 1 integrated over Q^2. The results for the elastic case are cross-checked with the calculation from STARlight MC and a good agreement between the fiducial cross-sections is found: $\sigma^{\rm el}_{fid} = 17.5$ nb, whereas $\sigma^{\rm STARlight}_{fid} = 17.0$ nb. Both calculations are also corrected by a factor $S^2 = 0.96$ which is calculated using STARlight, where the hard-sphere proton–nucleus requirement [24] is used.

Next, for the inelastic case ($\gamma p \to \ell^+\ell^- + X$), several recent parameterizations of the photon parton distributions are studied: CT14qed [15], HKR16qed [29], LUXqed17 [40] and NNPDF3.1luxQED [30]. One should note that all of these PDF sets include both elastic and inelastic parts of the photon spectrum. All predictions are scaled by $S^2 = 0.95$, again derived from STARlight. The integrated fiducial cross-sections for $p + \mathrm{Pb} \to \mathrm{Pb} + \ell^+\ell^- + X$ production at $\sqrt{s_{NN}} = 8.16$ TeV for different collinear photon PDF sets are summarized in Tab. II. Comparison of several lepton kinematic distributions between different photon-PDFs is shown in Fig. 2, including invariant mass and rapidity of lepton pair, and single-lepton transverse momentum/pseudorapidity distributions. The asymmetry visible on pair rapidity and single-lepton pseudorapidity distributions is due to expermental setup, which assumes a difference in the energy per nucleon between the proton beam and the lead beam (see Sec. III). All photon PDF parameterizations agree within 10% with each other. The small differences are mainly due to overall PDF normalization, as no change in the shape of various kinematic distributions is observed.

V. RESULTS INCLUDING PHOTON TRANSVERSE MOMENTUM

Several different parametrizations of proton strucure functions are used. Those are labeled as:

- ALLM [41, 42]: This parametrization gives a good fit to F_2 in most of the measured regions.

- FJLLM [43]: This parametrization explicitly includes the nucleon resonances and provides very good descripton of the CLAS data [44].

Contribution	$p_T^\ell > 4$ GeV	$p_T^\ell > 4$ GeV, $\lvert\eta^\ell\rvert < 2.4$, $m_{\ell^+\ell^-} > 10$ GeV
$\gamma_{\rm el}^p$	44.9(1) nb	17.5(1) nb
$\gamma_{\rm el}^p + \gamma_{\rm inel}^p$ [CT14qed_inc]	98.0(1) nb	39.7(1) nb
$\gamma_{\rm el}^p + \gamma_{\rm inel}^p$ [LUXqed17]	105.8(1) nb	44.1(1) nb
$\gamma_{\rm el}^p + \gamma_{\rm inel}^p$ [NNPDF3.1luxQED]	115.6(1) nb	45.9(1) nb
$\gamma_{\rm el}^p + \gamma_{\rm inel}^p$ [HKR16qed]	121.6(1) nb	49.4(1) nb

TABLE II: Integrated fiducial cross sections for $p + \mathrm{Pb} \to \mathrm{Pb} + \ell^+\ell^- + X$ production at $\sqrt{s_{NN}} =$ 8.16 TeV for different collinear photon PDF sets. An effect of applying only p_T^ℓ requirement is shown in second column. For comparison, the cross section for purely elastic contribution is also shown.

- SY [45]: This parameterization of Suri and Yennie from the early 1970's does not include DGLAP evolution. It is still used as one of the defaults in the LPAIR event generator [46].
- SU [47]: A parametrization which concentrates to give a good description at smal and intermediate Q^2 at not too small x. At large Q^2, it is complemented by the NNLO calculation of F_2 and F_L from NNLO MSTW 2008 PDF analysis [48].
- LUX-like: a recently constructed parametrization, described in details in Ref. [13]. This setup closely follows the LUXqed work from Ref.[40].

Table III shows the comparison of integrated fiducial cross sections for inelastic $p+\mathrm{Pb} \to \mathrm{Pb} + \ell^+\ell^- + X$ production at $\sqrt{s_{NN}} = 8.16$ TeV for different proton structure functions used. All structure functions provide similar fiducial cross-section, at the level of 16–18 nb. These inelastic cross-sections are also similar in size to the elastic contribution (18 nb) and are slightly lower than the numbers from collinear analysis, subtracted for elastic part (Table II).

Figure 3 presents differential cross sections for several lepton kinematic distributions: invariant mass of lepton pair, leading lepton transverse momentum, lepton pseudorapidity difference and leading lepton pseudorapidity. The shapes of the distributions obtained with various proton structure functions are very similar. For completeness, differential cross

Contribution	$p_T^\ell > 4$ GeV	$p_T^\ell > 4$ GeV, $\lvert\eta^\ell\rvert < 2.4$, $m_{\ell^+\ell^-} > 10$ GeV
$\gamma^p_{\rm el}$	47,89 nb	18.26 nb
$\gamma^p_{\rm inel}$ [LUX-like F2+FL]	42.57 nb	17.07 nb
$\gamma^p_{\rm inel}$ [LUX-like F2]	43.58 nb	17.44 nb
$\gamma^p_{\rm inel}$ [ALLM97 F2]	41.72 nb	16.43 nb
$\gamma^p_{\rm inel}$ [FJLLM F2]	45.24 nb	18.36 nb
$\gamma^p_{\rm inel}$ [SU F2]	41.72 nb	16.70 nb
$\gamma^p_{\rm inel}$ [SY F2]	40.38 nb	15.99 nb

TABLE III: Integrated fiducial cross sections for inelastic $p + \text{Pb} \to \text{Pb} + \ell^+\ell^- + X$ production at $\sqrt{s_{NN}} = 8.16$ TeV for different structure functions. An effect of applying only p_T^ℓ requirement is shown in second column.

sections as a function of lepton pair transverse momentum and azimuthal angle difference between the pair are shown in Fig. 4. Quite large (small) transverse momenta (angle differences) are possible, in contrast to leading-order calculations with collinear photons where the corresponding distributions are just a Dirac delta functions. The k_T-factorization approach should be considered more appropriate here. It is also visible that the SY parametrization gives lower predictions at larger pair-p_T, comparing to the other parametrizations used. This is because SY parametrization does not include explicit DGLAP evolution terms, which are appropriate at large photon virtualities.

Based on Fig. 4, it is also possible to separate experimentally the elastic part ($p + \text{Pb} \to p + \text{Pb} + \ell^+\ell^-$) with striking back-to-back topology, out of the inelastic contribution.

With k_T-factorization, one can also calculate the mass of the proton remnants. This is shown in Fig. 5, where the similar properties are observed (as in Fig. 4).

VI. DISCUSSION

We take the opportunity to calculate expected number of events for realistic assumption on total integrated luminosity. based on the previous pPb runs at the LHC, we assume $\int L dt = 200$ nb^{-1}.

(show some table(s) here)

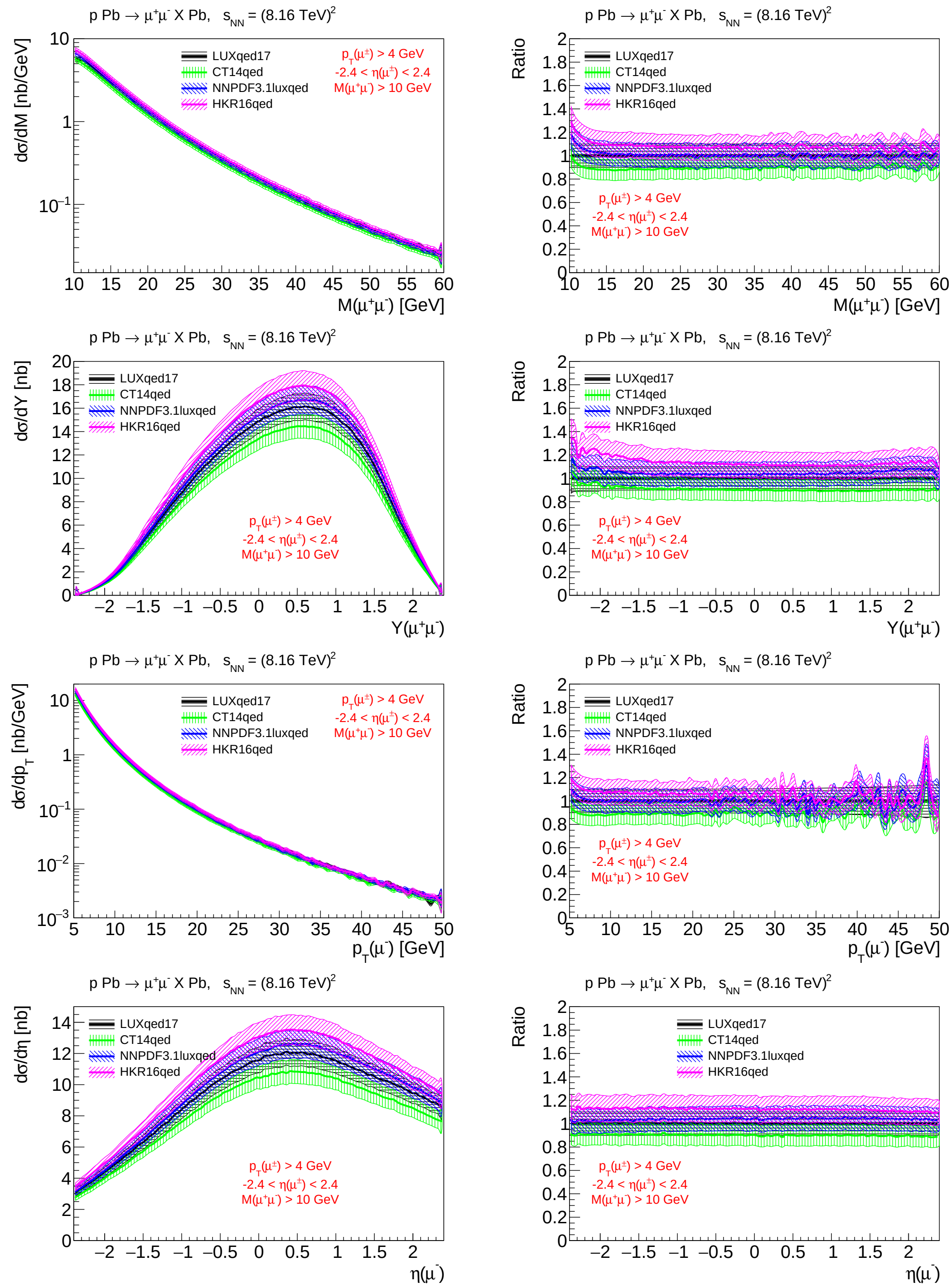

FIG. 2: Differential cross sections in the fiducial region for $p + \text{Pb} \to \text{Pb} + \ell^+\ell^- + X$ production at $\sqrt{s_{NN}} = 8.16$ TeV for different collinear photon PDF sets. Four differential distributions are shown (from top to bottom): invariant mass of lepton pair, pair rapidity, transverse momentum of negatively-charged lepton and its pseudorapidity. Figures on the right show the ratios to LUXqed17 PDF.

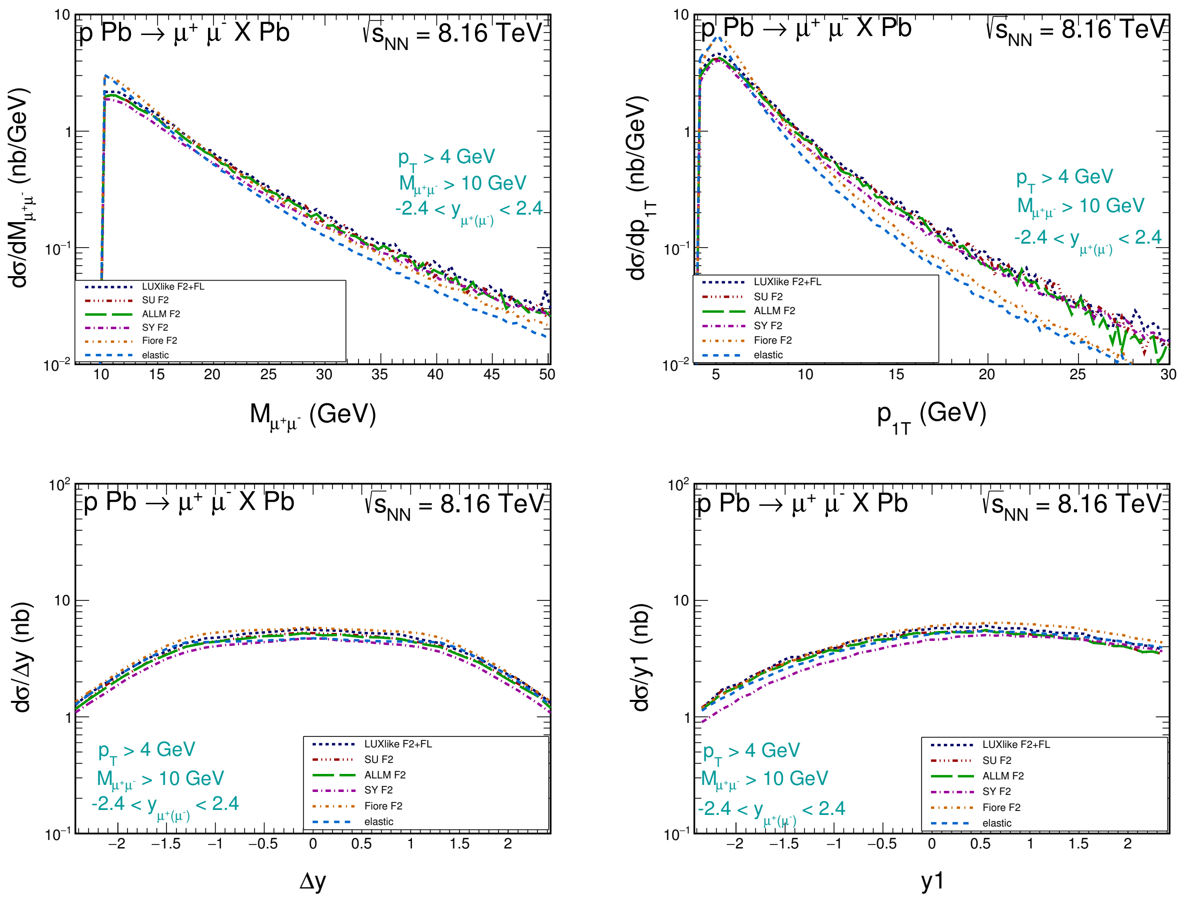

FIG. 3: Differential cross sections in the fiducial region for $p + \mathrm{Pb} \to \mathrm{Pb} + \ell^+\ell^- + X$ production at $\sqrt{s_{NN}} = 8.16$ TeV in k_T factorization approach for several proton structure functions. Four differential distributions are shown: invariant mass of lepton pair (top left), leading lepton transverse momentum (top right), lepton pseudorapidity difference (bottom left) and leading lepton pseudorapidity (bottom right). For comparison, the elastic contribution ($p + \mathrm{Pb} \to p + \mathrm{Pb} + \ell^+\ell^-$) is also shown.

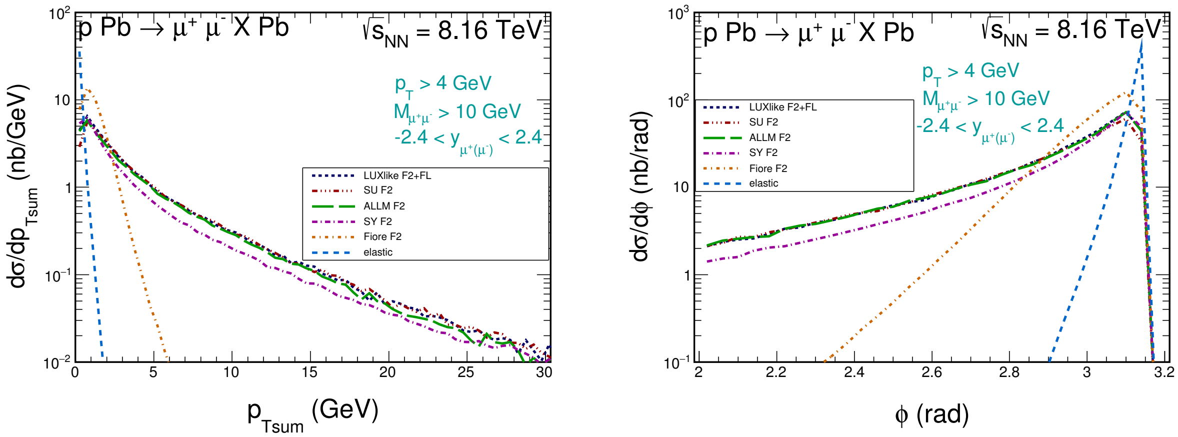

FIG. 4: Differential cross sections in the fiducial region for $p + \mathrm{Pb} \to \mathrm{Pb} + \ell^+\ell^- + X$ production at $\sqrt{s_{NN}} = 8.16$ TeV in k_T factorization approach for several proton structure functions. Two differential distributions are shown: transverse momentum of lepton pair (left) and azimuthal angle difference between the pair (right). For comparison, the elastic contribution ($p + \mathrm{Pb} \to p + \mathrm{Pb} + \ell^+\ell^-$) is also shown.

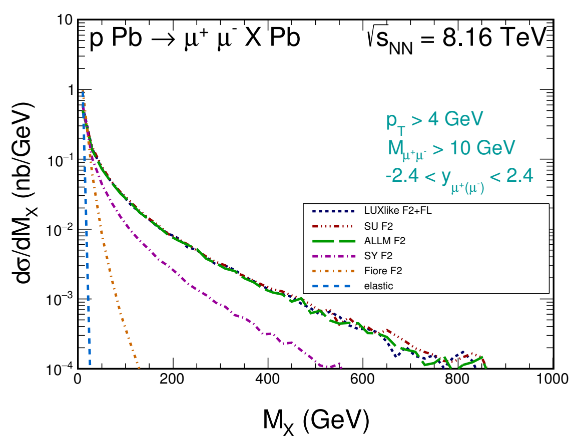

FIG. 5: Differential cross section as a function of the mass of the proton remnants in the fiducial region for $p+\mathrm{Pb} \to \mathrm{Pb}+\ell^+\ell^-+X$ production at $\sqrt{s_{NN}} = 8.16$ TeV in k_T factorization approach for several proton structure functions. For comparison, the elastic contribution ($p+\mathrm{Pb} \to p+\mathrm{Pb}+\ell^+\ell^-$) is also shown.

VII. SUMMARY

In summary, we propose a method that would unambiguously allow to test and constrain the photon parton distribution at LHC energies. This method is based on the measurement of the cross-section for the reaction $p+\mathrm{Pb} \rightarrow \mathrm{Pb}+\ell^+\ell^-+X$, where the expected background is small comparing to the analogous process in *pp* collisions. Results are shown for different choices of collinear photon PDFs, and a comparison is made with unintegrated photon distributions that include non-zero photon transverse momentum. For collinear approach and by analogy to DIS, the correct choice of the scale is identified. Using simple (realistic) experimental requirements on lepton kinematics, it is shown that one can expect O(X) events with the existing datasets recorded by ATLAS/CMS at $\sqrt{s_{NN}} = 8.16$ TeV for each lepton flavour.

References

---

[1] ATLAS Collaboration, G. Aad et al., *Measurement of the low-mass Drell-Yan differential cross section at $\sqrt{s} = 7$ TeV using the ATLAS detector*, JHEP **06** (2014) 112, arXiv:1404.1212 [hep-ex].

[2] ATLAS Collaboration, G. Aad et al., *Measurement of the double-differential high-mass Drell-Yan cross section in pp collisions at $\sqrt{s} = 8$ TeV with the ATLAS detector*, JHEP **08** (2016) 009, arXiv:1606.01736 [hep-ex].

[3] E. Accomando, J. Fiaschi, F. Hautmann, S. Moretti, and C. H. Shepherd-Themistocleous, *Photon-initiated production of a dilepton final state at the LHC: Cross section versus forward-backward asymmetry studies*, Phys. Rev. **D95** (2017) no. 3, 035014, arXiv:1606.06646 [hep-ph].

[4] M. Luszczak, W. Schafer, and A. Szczurek, *Two-photon dilepton production in proton-proton collisions: two alternative approaches*, Phys. Rev. **D93** (2016) no. 7, 074018, arXiv:1510.00294 [hep-ph].

[5] L. A. Harland-Lang, V. A. Khoze, and M. G. Ryskin, *The photon PDF in events with rapidity gaps*, Eur. Phys. J. **C76** (2016) no. 5, 255, arXiv:1601.03772 [hep-ph].

[6] M. Luszczak, A. Szczurek, and C. Royon, *W^+W^- pair production in proton-proton collisions: small missing terms*, JHEP **02** (2015) 098, `arXiv:1409.1803 [hep-ph]`.

[7] A. Denner, S. Dittmaier, M. Hecht, and C. Pasold, *NLO QCD and electroweak corrections to $Z+\gamma$ production with leptonic Z-boson decays*, JHEP **02** (2016) 057, `arXiv:1510.08742 [hep-ph]`.

[8] M. Dyndal and L. Schoeffel, *Four-lepton production from photon-induced reactions in pp collisions at the LHC*, Acta Phys. Polon. **B47** (2016) 1645, `arXiv:1511.02065 [hep-ph]`.

[9] M. Ababekri, S. Dulat, J. Isaacson, C. Schmidt, and C. P. Yuan, *Implication of CMS data on photon PDFs*, `arXiv:1603.04874 [hep-ph]`.

[10] B. Biedermann, M. Billoni, A. Denner, S. Dittmaier, L. Hofer, B. Jger, and L. Salfelder, *Next-to-leading-order electroweak corrections to $pp \to W^+W^- \to 4$ leptons at the LHC*, JHEP **06** (2016) 065, `arXiv:1605.03419 [hep-ph]`.

[11] B. Biedermann, A. Denner, S. Dittmaier, L. Hofer, and B. Jger, *Electroweak corrections to $pp \to \mu^+\mu^-e^+e^- + X$ at the LHC: a Higgs background study*, Phys. Rev. Lett. **116** (2016) no. 16, 161803, `arXiv:1601.07787 [hep-ph]`.

[12] Y. Wang, R.-Y. Zhang, W.-G. Ma, X.-Z. Li, and L. Guo, *QCD and electroweak corrections to ZZ+jet production with Z -boson leptonic decays at the LHC*, Phys. Rev. **D94** (2016) no. 1, 013011, `arXiv:1604.04080 [hep-ph]`.

[13] M. Luszczak, W. Schafer, and A. Szczurek, *Production of W^+W^- pairs via $\gamma^*\gamma^* \to W^+W^-$ subprocess with photon transverse momenta*, JHEP **05** (2018) 064, `arXiv:1802.03244 [hep-ph]`.

[14] A. Manohar, P. Nason, G. P. Salam, and G. Zanderighi, *How bright is the proton? A precise determination of the photon parton distribution function*, Phys. Rev. Lett. **117** (2016) no. 24, 242002, `arXiv:1607.04266 [hep-ph]`.

[15] C. Schmidt, J. Pumplin, D. Stump, and C. P. Yuan, *CT14QED parton distribution functions from isolated photon production in deep inelastic scattering*, Phys. Rev. **D93** (2016) no. 11, 114015, `arXiv:1509.02905 [hep-ph]`.

[16] NNPDF Collaboration, R. D. Ball, V. Bertone, S. Carrazza, L. Del Debbio, S. Forte, A. Guffanti, N. P. Hartland, and J. Rojo, *Parton distributions with QED corrections*, Nucl. Phys. **B877** (2013) 290–320, `arXiv:1308.0598 [hep-ph]`.

[17] xFitter Developers' Team Collaboration, F. Giuli et al., *The photon PDF from high-mass*

Drell-Yan data at the LHC, Eur. Phys. J. **C77** (2017) no. 6, 400, `arXiv:1701.08553 [hep-ph]`.

[18] ATLAS Collaboration, G. Aad et al., *Measurement of exclusive $\gamma\gamma \to \ell^+\ell^-$ production in proton-proton collisions at $\sqrt{s} = 7$ TeV with the ATLAS detector*, Phys. Lett. **B749** (2015) 242–261, `arXiv:1506.07098 [hep-ex]`.

[19] ATLAS Collaboration, M. Aaboud et al., *Measurement of the exclusive $\gamma\gamma \to \mu^+\mu^-$ process in proton-proton collisions at $\sqrt{s} = 13$ TeV with the ATLAS detector*, Phys. Lett. **B777** (2018) 303–323, `arXiv:1708.04053 [hep-ex]`.

[20] CMS Collaboration, S. Chatrchyan et al., *Exclusive photon-photon production of muon pairs in proton-proton collisions at $\sqrt{s} = 7$ TeV*, JHEP **01** (2012) 052, `arXiv:1111.5536 [hep-ex]`.

[21] CMS Collaboration, S. Chatrchyan et al., *Search for exclusive or semi-exclusive photon pair production and observation of exclusive and semi-exclusive electron pair production in pp collisions at $\sqrt{s} = 7$ TeV*, JHEP **11** (2012) 080, `arXiv:1209.1666 [hep-ex]`.

[22] CMS, TOTEM Collaboration, A. M. Sirunyan et al., *Observation of proton-tagged, central (semi)exclusive production of high-mass lepton pairs in pp collisions at 13 TeV with the CMS-TOTEM precision proton spectrometer*, JHEP **07** (2018) 153, `arXiv:1803.04496 [hep-ex]`.

[23] V. M. Budnev, I. F. Ginzburg, G. V. Meledin, and V. G. Serbo, *The two photon particle production mechanism. Physical problems. Applications. Equivalent photon approximation*, Phys. Rept. **15** (1975) 181.

[24] S. R. Klein, J. Nystrand, J. Seger, Y. Gorbunov, and J. Butterworth, *STARlight: A Monte Carlo simulation program for ultra-peripheral collisions of relativistic ions*, Comput. Phys. Commun. **212** (2017) 258–268, `arXiv:1607.03838 [hep-ph]`.

[25] M. Gluck, C. Pisano, and E. Reya, *The Polarized and unpolarized photon content of the nucleon*, Phys. Lett. **B540** (2002) 75–80, `arXiv:hep-ph/0206126 [hep-ph]`.

[26] A. D. Martin, R. G. Roberts, W. J. Stirling, and R. S. Thorne, *Parton distributions incorporating QED contributions*, Eur. Phys. J. **C39** (2005) 155–161, `arXiv:hep-ph/0411040 [hep-ph]`.

[27] A. D. Martin and M. G. Ryskin, *The photon PDF of the proton*, Eur. Phys. J. **C74** (2014) 3040, `arXiv:1406.2118 [hep-ph]`.

[28] C. Schmidt, J. Pumplin, D. Stump, and C. P. Yuan, *QED effects and Photon PDF in the CTEQ-TEA Global Analysis*, PoS **DIS2014** (2014) 054.

[29] L. A. Harland-Lang, V. A. Khoze, and M. G. Ryskin, *Photon-initiated processes at high mass*, Phys. Rev. **D94** (2016) no. 7, 074008, arXiv:1607.04635 [hep-ph].

[30] NNPDF Collaboration, V. Bertone, S. Carrazza, N. P. Hartland, and J. Rojo, *Illuminating the photon content of the proton within a global PDF analysis*, SciPost Phys. **5** (2018) 008, arXiv:1712.07053 [hep-ph].

[31] G. G. da Silveira, L. Forthomme, K. Piotrzkowski, W. Schfer, and A. Szczurek, *Central production via photon-photon fusion in proton-proton collisions with proton dissociation*, JHEP **02** (2015) 159, arXiv:1409.1541 [hep-ph].

[32] ATLAS Collaboration, G. Aad et al., *The ATLAS Experiment at the CERN Large Hadron Collider*, JINST **3** (2008) S08003.

[33] CMS Collaboration, S. Chatrchyan et al., *The CMS Experiment at the CERN LHC*, JINST **3** (2008) S08004.

[34] S. D. Drell and T.-M. Yan, *Massive Lepton Pair Production in Hadron-Hadron Collisions at High-Energies*, Phys. Rev. Lett. **25** (1970) 316–320. [Erratum: Phys. Rev. Lett.25,902(1970)].

[35] ATLAS Collaboration, G. Aad et al., *Z boson production in p+Pb collisions at* $\sqrt{s_{NN}} = 5.02$ *TeV measured with the ATLAS detector*, Phys. Rev. **C92** (2015) no. 4, 044915, arXiv:1507.06232 [hep-ex].

[36] CMS Collaboration, V. Khachatryan et al., *Study of Z boson production in pPb collisions at* $\sqrt{s_{NN}} = 5.02$ *TeV*, Phys. Lett. **B759** (2016) 36–57, arXiv:1512.06461 [hep-ex].

[37] ALICE Collaboration, J. Adam et al., *W and Z boson production in p-Pb collisions at* $\sqrt{s_{\mathrm{NN}}}$ *= 5.02 TeV*, JHEP **02** (2017) 077, arXiv:1611.03002 [nucl-ex].

[38] ALICE Collaboration, G. Dellacasa et al., *ALICE technical design report of the zero degree calorimeter (ZDC)*, . CERN-LHCC-99-05.

[39] ATLAS Collaboration, *Zero degree calorimeters for ATLAS*, . CERN-LHCC-2007-01.

[40] A. V. Manohar, P. Nason, G. P. Salam, and G. Zanderighi, *The Photon Content of the Proton*, JHEP **12** (2017) 046, arXiv:1708.01256 [hep-ph].

[41] H. Abramowicz, E. M. Levin, A. Levy, and U. Maor, *A Parametrization of sigma-T (gamma* p) above the resonance region* $Q^2 \geq 0$, Phys. Lett. **B269** (1991) 465–476.

[42] H. Abramowicz and A. Levy, *The ALLM parameterization of sigma(tot)(gamma* p): An Update*, arXiv:hep-ph/9712415 [hep-ph].

[43] R. Fiore, A. Flachi, L. L. Jenkovszky, A. I. Lengyel, and V. K. Magas, *Explicit model realizing parton hadron duality*, Eur. Phys. J. **A15** (2002) 505–515, arXiv:hep-ph/0206027 [hep-ph].

[44] CLAS Collaboration, M. Osipenko et al., *A Kinematically complete measurement of the proton structure function F(2) in the resonance region and evaluation of its moments*, Phys. Rev. **D67** (2003) 092001, arXiv:hep-ph/0301204 [hep-ph].

[45] A. Suri and D. R. Yennie, *The space-time phenomenology of photon absorption and inelastic electron scattering*, Annals Phys. **72** (1972) 243.

[46] J. A. M. Vermaseren, *Two Photon Processes at Very High-Energies*, Nucl. Phys. **B229** (1983) 347–371.

[47] A. Szczurek and V. Uleshchenko, *Nonpartonic components in the nucleon structure functions at small Q^2 in the broad range of x*, Eur. Phys. J. **C12** (2000) 663–671, arXiv:hep-ph/9904288 [hep-ph].

[48] A. D. Martin, W. J. Stirling, R. S. Thorne, and G. Watt, *Parton distributions for the LHC*, Eur. Phys. J. **C63** (2009) 189–285, arXiv:0901.0002 [hep-ph].